JOURNAL OF MAGNETIC RESONANCE **129,** 188–200 (1997)
ARTICLE NO. MN971248

Analysis of the Movement of Line-like Samples of Variable Length along the *X*-Axis of a Double TE_{104} and a Single TE_{102} Rectangular Cavity

Milan Mazúr,*[,1] Harry Morris,† and Marián Valko*

**Department of Physical Chemistry, Faculty of Chemical Technology, Slovak Technical University, Radlinského 9, SK-812 37 Bratislava, Slovakia; and †School of Pharmacy and Chemistry, Liverpool John Moores University, Byrom Street, Liverpool L3 3AF, United Kingdom*

Received March 18, 1997; revised July 10, 1997

Movement of line-like samples with lengths from 5 to 50 mm along the *x*-axis of the double TE_{104} rectangular cavity has been analyzed. The observed dependencies of the EPR signal intensity versus sample position showed: (i) a sharp maximum for sample lengths from 5 to 20 mm; (ii) a plateau, over which the EPR signal intensity remained constant within experimental errors of 0.26–1.07%, for lengths from 30 to 40 mm; and (iii) a "sloping plateau," which could be approximated by the linear function (correlation, $r = 0.98$) for sample length 50 mm. Theoretical values of the experimentally observed dependencies of the intensity versus sample position were calculated using the modified sine-squared function and the correlation between observed and theoretically predicted dependencies is very good. The experimental dependence of the EPR signal intensity versus the sample length for samples situated at the same point in the cavity was nonlinear with a maximum for the 40-mm sample. The dependence of the EPR signal intensity upon the movement of a large cylindrical sample (o.d. 4 mm and length 100 mm) along the *x*-axis of the cavity was similar to that found for the 50-mm sample. However, an additional oscillating signal superimposed on the sloping plateau was observed. The presence of a large sample fixed in the complementary cavity of the double TE_{104} cavity caused an additional deformation of the signal intensity for a 30-mm sample which was moving in the first cavity. The primary effect was that the plateau was replaced by a region in which the intensity increased linearly with sample position, $r = 0.99$. Each of the above phenomena may be a source of significant errors in quantitative EPR spectroscopy. Cylindrical samples to be compared should be of identical length and internal diameter. Accurate and precise positioning of each sample in the microwave cavity is essential.

Key Words: **quantitative EPR spectroscopy; double and single cavity; sample length.**

INTRODUCTION

Difficulties encountered in quantifying EPR spectroscopic measurements were clearly demonstrated in the results obtained from international experiments carried out in 1962 (*1*) and 1991–1992 (*2*). In principle, experimental errors in quantitative EPR measurements for a given laboratory and a given EPR spectrometer may be reduced in carefully performed experiments to between 2 and 5% (*3–10*). However, in practice, experimental analysis of the same sample in different laboratories produced results which in the worst cases were incompatible and in others had an uncertainty of between 100 and 200% (*1, 5*), and others up to 500% (*4*). No satisfactory explanation for this discrepancy has been found at present.

In Parts 1 and 2 of this series (*11, 12*), it was shown that the correct comparison of two samples (sample and reference) in the TE_{104} double cavity could be obtained only if either the influence of both samples on the microwave and modulation fields are negligibly small or both halves of the cavity have the same microwave properties (*2, 5, 13–22*). This is valid only under ideal experimental conditions in which both samples have the same size, shape, and magnetic susceptibility and are placed at the same position within the microwave cavity. These criteria are in practice only fulfilled for a point-like sample (*4, 5, 13–19*). However, samples used for quantitative EPR investigations are frequently not point-like and in practice the sample/standard is usually contained in a thin-walled quartz tube (3 or 4 mm o.d.), which is filled by the liquid, or powdered material to produce column lengths varying from 5 to 50 mm or more. These cylindrical samples are then positioned as near as possible to the center of the cavity with more or less accuracy (*2, 5, 17–19*).

In quantitative EPR it is sometimes necessary to compare the unknown cylindrical sample (with a variable length) either to small (point-like) samples or to commercially available full-length cavity standard samples (e.g., pitch in KCl contained in a quartz tube with o.d. about 4 mm). Significant systematic errors may occur in such quantitative measurements, and true comparison of the experimental data from the same samples, but obtained from different EPR laboratories, may be very problematic (*2, 5, 18, 19*). This led us to the investigation described in this paper.

[1] To whom correspondence should be addressed. Fax: (+421 7) 393 198. E-mail: mazur@cvt.stuba.sk.

1090-7807/97 $25.00

In the first part of this series (*11*) the construction of a new sample setup device for precisely inserting the reference and unknown sample into the center of the TE_{104} double rectangular cavity was described. In the second part (*12*) a detailed analysis of the sample- and double TE_{104} cavity-associated errors was described; and the movement of full-length cavity line-like samples into the double TE_{104} cavity was investigated. The aim of this paper is the detailed analysis of the movement of line-like samples with differing column lengths and diameters into the double TE_{104} cavity. The sources of error caused by the comparison of such samples are discussed. This involved the recording and analysis of over 1000 spectra.

EXPERIMENTAL

The samples were prepared and measured according to the same procedures as described in the experimental section of the previous paper (*12*) of this series. A short recapitulation, with specific reference to the preparation and measurement of line-like samples with various lengths, is described.

Sample preparation. Line-like samples of length L were prepared as follows: The original tube (o.d. $\approx$ 4 mm) containing the standard powdered strong pitch sample was opened under an inert atmosphere and the material reloaded into thin-walled quartz EPR tubes (i.d. 1.3 mm, length 60 mm, wall thickness $\approx$ 0.1 mm) to produce pairs of identical (verified by weighing) line-like samples with material lengths from 5 to 50 mm, which were then sealed under gentle vacuum. The basic procedure for sample filling the sample tubes was as follows: The powdered material was poured in the sample tube, shaken, and pressed carefully by lightly knocking the tube on the laboratory table 10 times. Additional material was added if necessary to give the desired sample length. The experimental errors (SD in %) of the volume weight of the powder samples with given length prepared using this filling procedure were about 0.5% or less (*12*). Pairs of the identical (again verified by weighing) point-like samples were prepared by making cylindrical samples with a material column length 1.3 mm and i.d. 1.3 mm in the manner described above. The large cylindrical sample was realized using the commercially available standard ''strong pitch in KCl'' sample in the original tube (o.d. $\approx$ 4 mm, $L \approx 100$ mm). In this case the sample alignment procedure was modified as described in the first part of this series (*11*).

Apparatus, instrumental parameters, and EPR signal intensity expression. Spectra were recorded using a Bruker ER 200 D-SRC with an Aspect computer EPR spectrometer with the original double TE_{104} (the first cavity is defined as the front cavity) and single TE_{102} rectangular cavity (*23*). Instrumental parameters identical to those described in the previous paper were used (*12*). The temperature of the EPR laboratory was regulated at 16°C.

In all cases the intensity of the EPR signal was characterized by the peak-to-peak height of the first-derivative EPR signal, I_{pp}. For convenience of analysis, all I_{pp} values were normalized to the interval $\langle 0, 1 \rangle$. Statistical evaluation of the data obtained was carried out according to standard statistical procedures.

MAPPING OF THE SAMPLE MOVEMENT IN A RECTANGULAR CAVITY

The location of the origin and axis orientation of the microwave rectangular cavity- and line-like sample-based coordinate systems and the definition and designation of the important sample- and cavity-connected points are given in Fig. 1 of Part 2 of this series (*12*). Only a short recapitulation with particular reference to the movement of the samples in the rectangular cavity is given. Since the y- and z- coordinates are zero in all of the cases under investigation, only the x-coordinate of the sample- and cavity-connected points is shown.

The center of line-like sample of length L situated in the center of the rectangular cavity is defined as follows: $S_c(L/2) \equiv P_c(0)$. L_{ef} is the effective length of the sample, namely, that part of the total sample length, L, which is situated in the active part, length a, of the microwave cavity (for the TE_{104} cavity, $a = 23.5$ mm). If $L < a$ then $L_{ef} = L$, and if $L \geq a$ then $L_{ef} = a$. L_{pl} is the residual part of the sample length, L, which is not situated in the active part of the microwave cavity. If $L \leq a$ then $L_{pl} = 0$, and if $L > a$ then $L_{pl} = L - a$.

Line-like Sample Position in the Cavity

Figure 1 shows the sample and cavity reference points for the different situations which can arise from positioning line-like samples in the rectangular cavity: Fig. 1a)—the case of a point-like sample, a line-like sample with $L \to 0$; Figs. 1b ($L < a$), 1c ($L = a$), and 1d to 1f ($L > a$)—the cases for line-like samples. In the limiting case (Fig. 1a), if $L \to 0$, then $S_c(L/2) \to S_0(0)$, which is compatible with the position of a point-like sample, then $S_0(0) \equiv P_c(0)$. See, for example, (*5, 13, 17, 18*).

The sample position (Fig. 1b) for $L < a$ and (Fig. 1c) for $L = a$ is again straightforward, giving $L_{ef} = L$ and $L_{ef} = a$, respectively. If $L = a$, then $S_c(L/2) \equiv S_c(a/2)$, which is an important boundary case for a line-like sample with central position $S_c(L/2) \equiv S_c(a/2) \equiv P_c(0)$.

The case $L > a$ (line-like sample with nonzero residual length L_{pl}) is rather complicated, and it is useful to introduce two further sample reference points: (i) the situation (Fig. 1d), $S_0(0) \equiv P_{out}(-a/2)$, in which the first auxiliary center of the sample is (S'_c), for which $S'_c(L_{ef}/2) \equiv S'_c(a/2) \equiv P_c(0)$ is valid; and (ii) the situation (Fig. 1f) $S_L(L) \equiv P_{in}(a/2)$, in which the second auxiliary center of the sample is S''_c, for which $S''_c((L - L_{ef})/2) \equiv S''_c(L - a/2) \equiv P_c(0)$ is valid.

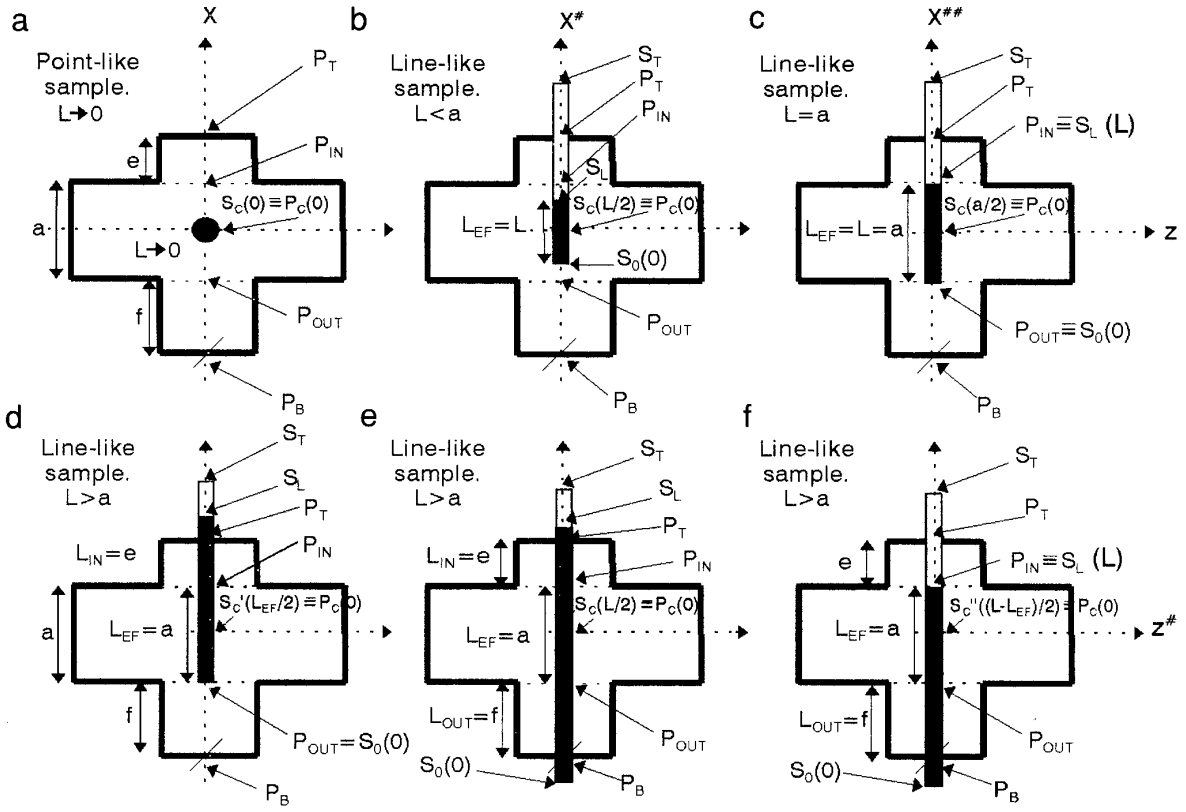

FIG. 1. Schematic diagram of the different positions of a line-like sample of variable length, L, in the rectangular cavity: (a) Point-like sample, $L \to 0$. (b) Line-like sample, $L < a$. (c) Line-like sample, $L = a$. (d)–(f) Line-like sample, $L > a$. (For the symbol abbreviations and a more detailed description see text.)

Central positioning of the sample, $L > a$, at the cavity center is clear from the definition $S_c(L/2) \equiv P_c(0)$ (see Fig. 1e). However, the nonzero value for L_{pl} results in a constant I_{pp} value (the so-called plateau) in the interval of the sample movement from the starting position $S'_c(L_{ef}/2) \equiv P_c(0)$ (see Fig. 1d) to the position $S''_c((L - L_{ef})/2) \equiv P_c(0)$ (see Fig. 1f) in the cavity. The position $S_c(L/2) \equiv P_c(0)$ is the central position on the plateau.

The possible contributions of the EPR signals from the sample ends positioned at both the top, e, and the bottom, f, sample access holes (i.e., those parts of the cavity between the P_T and P_{in}, and P_{out} and P_B points, respectively) to the main EPR signal, from that part of the sample situated in the active part of the cavity, was assumed nonzero as suggested by Barklie and Sealy (*17*).

In order to precisely analyze the sample movement in the rectangular cavity, further points (A–F) on the theoretically predicted and experimentally observed I_{pp} dependencies were defined as given in Table 1. The second row of the table shows the cavity points relative to the sample points S_0, S_c, and S_L, during the sample movement in the cavity. The coordinates of the cavity-based points $P(*)$ are expressed in both the x- and the x'-axes for a point-like sample and for the three cases of line-like samples in the following rows while the last row shows the coordinates of the points used for the construction of the theoretical sine-squared function with a plateau using the special $*x'$-, x''- and x'''-axes. See Appendix A for further details.

The x-axis of the sample-based coordinate system was not transformed during the sample movement along the common sample–cavity x-axis; therefore, it was necessary to introduce two different x-axes for the cavity-based coordinate systems: (i) the x-axis used with the experimentally observed I_{pp} value dependencies and (ii) the x'-axis used with the theoretically predicted I_{pp} value dependencies. The linear transformation between the two systems is $x = x' + L/2$ (see Fig. 1 and Table 1). In order to compare the experimentally observed and the theoretically predicted I_{pp} values the theoretical dependencies were transformed from the x'- to the x-axis.

Sine-Squared Function for Line-like Sample with Variable Length, L

The theoretically predicted variation of the I_{pp} values with movement of a point-like sample along the x-axis of the microwave rectangular cavity was calculated according to the literature (*13, 17*) using the equation of Barklie and

TABLE 1

Definition of the Sample (*S*)- and Cavity (*P*)-Based Points, Which Are Important in the Analysis of the Movement of Line-like Samples with a Variable Length, *L*, along the Common Sample–Cavity *x*-Axis of the Rectangular Cavity

Important points:	*A*	*B*	**C*	*C*′*D*′	**D*	*E*	*F*	Transformation between **x**- and **x**′-axis	*Note.* Points **C*, **D* are valid only for $\mathbf{L} > \mathbf{a}$.
If sample-connected points ≡ cavity-connected points	$S_0(0) \equiv P_{in}(*)$	$S_0(0) \equiv P_c(*)$	$S_0(0) \equiv P_{out}(*)$	$S_c(L/2) \equiv P_c(*)$	$S_c(L) \equiv P_{in}(*)$	$S_L(L) \equiv P_c(*)$	$S_L(L) \equiv P_{out}(*)$		
P(*) coordinate for									*Note.* For $\mathbf{L} = \mathbf{0}$ $B = C'D' = E$ is valid.
(i) Point-like sample $\mathbf{L} = \mathbf{0}$									
x-axis	$-a/2$	0	—	0	—	0	$a/2$	$x = x' + L/2$	
x′-axis	$-\mathbf{a/2}$	**0**	—	**0**	—	**0**	$\mathbf{a/2}$	$\mathbf{x}' = \mathbf{x} - \mathbf{L/2}$	
(ii) Line-like sample									*Note.* General formula for $\mathbf{L} \leq \mathbf{a}$.
(1) $\mathbf{L} < \mathbf{a}$									
x-axis	$-a/2$	0	—	$L/2$	—	L	$a/2 + L$	$x = x' + L/2$	
x′-axis	$-(\mathbf{a} + \mathbf{L})/\mathbf{2}$	$-\mathbf{L/2}$	—	**0**	—	$\mathbf{L/2}$	$(\mathbf{a} + \mathbf{L})/\mathbf{2}$	$\mathbf{x}' = \mathbf{x} - \mathbf{L/2}$	
(2) $\mathbf{L} = \mathbf{a}$									*Note.* For $\mathbf{L} = \mathbf{a}$ **C* = *C*′*D*′ = **D* is valid.
x-axis	$-a/2$	0	$a/2$	$a/2$	$a/2$	a	$3a/2$	$x = x' + L/2$	
x′-axis	$-\mathbf{a}$	$-\mathbf{a/2}$	**0**	**0**	**0**	$\mathbf{a/2}$	$\mathbf{a}$	$\mathbf{x}' = \mathbf{x} - \mathbf{L/2}$	
(3) $\mathbf{L} > \mathbf{a}$									*Note.* A plateau for $\mathbf{L} > \mathbf{a}$. See next a, b, c rows.
x-axis	$-a/2$	0	$a/2$	$L/2$	$L - a/2$	L	$a/2 + L$	$x = x' + L/2$	
x′-axis	$-(\mathbf{a} + \mathbf{L})/\mathbf{2}$	$-\mathbf{L/2}$	$-(\mathbf{L} - \mathbf{a})/\mathbf{2}$	0	$(\mathbf{L} - \mathbf{a})/\mathbf{2}$	$\mathbf{L/2}$	$(\mathbf{a} + \mathbf{L})/\mathbf{2}$	$\mathbf{x}' = \mathbf{x} - \mathbf{L/2}$	
Sine-squared function with plateau $\mathbf{L} > \mathbf{a}$								**x*′ = *x*′	*Note.* New auxiliary center: $S_c'(L_{ef}/2) = P_c(*)$
								$x'' = x' + (L - a)/2$	$*S_c(L/2) = P_c(*)S_c''$
(a) *x*″-axis	$-\mathbf{a}$	$-\mathbf{a/2}$	**0**	—	—	—	—	$x'' = x - a/2$	$((L - L_{ef})/2) = P_c(*)$
(b) **x*′-axis	—	—	$-(\mathbf{L} - \mathbf{a})/\mathbf{2}$	**0**	$(\mathbf{L} - \mathbf{a})/\mathbf{2}$	—	—	$x''' = x' - (L - a)/2$	
(c) *x*‴-axis	—	—	—	—	**0**	$\mathbf{a/2}$	$\mathbf{a}$	$x''' = x + a/2$	

Note. The coordinates of the cavity-connected *P*(*) points are expressed in both the *x*- and the *x*′-coordinate systems. The boundary values of the *x*′-coordinates used in the theoretical prediction of the I_{pp} values using the theoretical sine-squared function are displayed in bold. The special **x*′-, *x*″-, and *x*‴-coordinate systems were introduced for the construction of the theoretical sine-squared function with a plateau (for more details see text).

Sealy (*17*), viz., I_{pp} = const. $\sin^2[\pi/a(x + a/2)]$, the so-called sine-squared function in which a is the length of the active part of the cavity along the sample. This basic equation was modified for line-like samples with variable length L by increasing the active length of the cavity to $(a + L_{ef})$ as follows: (i) if $L < a$, then $L_{ef} = L$ and I_{pp} = const. $\sin^2[\pi/(a + L)(x + (a + L)/2)]$; (ii) if $L \geq a$ then $L_{ef} = a$ and I_{pp} = const. $\sin^2[\pi/2a(x + a)]$. However, if $L > a$, then a plateau of width $L_{pl} = L - a$ was expected, in which case the theoretical functions were constructed from ''left and right half'' of the sine-squared functions, which were then connected by a plateau of constant I_{pp} values, or by a linear function. See Appendixes A and B for further details.

Mapping of the Sample Movement in the Cavity

Figure 2 shows how the normalized, theoretically predicted I_{pp} values varied as a function of the movement of a point-like and line-like sample of length L along the common sample–cavity x-axis of the rectangular cavity. With reference to Figs. 1 and 2, Table 1, and Appendix A, the dependence of I_{pp} on the sample position in the rectangular cavity can be analyzed for each of the four cases described above:

(i) A point-like sample with $L \rightarrow 0$, Fig. 2a.

In this case the situation is relatively simple because $L \rightarrow 0$, $L_{ef} \rightarrow 0$, and $L_{pl} = 0$. The sample position in the center of the cavity is $S_L(0) \equiv S_c(0) \equiv S_0(0) \equiv P_c(0)$, or in the alternative notation $B \equiv C'D' \equiv E$ (see Fig. 1a and Table 1). The I_{pp} values varied from zero at point A $(-x' = -a/2)$, increased to a maximum at $B \equiv C'D' \equiv E$ $(-x' = 0)$, and then decreased to zero at point F $(-x' = a/2)$ in good accord with published literature data (*5, 13, 17, 18*). In this case the x- and x'- axes are identical ($x = x'$, because $L \rightarrow 0$) and it is clear that the x'-axis values varied from $-a/2$ to $a/2$ giving a sine-squared function width equal to ''a''. See Appendix A.

(ii) A line-like sample with $L \leq a$, Figs. 2b and 2c.

In this case, $L_{ef} = L$ and $L_{pl} = 0$, and no plateau is observed. The sample position in the center of the cavity is $P_c(0) \equiv S_c(L/2)$, or in the new notation the point $C'D'$. The I_{pp} values varied from zero at point A $(-x' = -(a + L)/2)$, increased to point B $(-x' = -L/2)$, and further increased to the maximum at $C'D'$ $(-x' = 0)$ from which they decrease through E $(-x' = L/2)$ to zero at F $(-x = (a + L)/2)$. In this case the x' values varied from $-(a + L)/2$ to $(a + L)/2$, and the sine-squared function width is equal to $(a + L)$. For the special case $L = a$ the function width is $2a$, with points B and E having values of 0.5 at $-x' = \pm a/2$, and this situation is an important boundary case for curves without, $*C = C'D' = *D$ $(-x' = 0)$, and with a plateau. See Appendix A.

(iii) A line-like sample with $L > a$, Fig. 2d.

In this case $L_{ef} = a$ and $L_{pl} = L - a$ $(= L - L_{ef})$, and a plateau is observed. The sample position in the center of the cavity is $P_c(0) \equiv S_c(L/2)$, at point $C'D'$ (compare Fig. 1e and Table 1). The I_{pp} values varied from zero at points F, A $(-x' = \pm(a + L)/2$, respectively), through points E, B $(-x' = \pm L/2)$, with a maximum at $*D$, $*C$ $(-x' = \pm(L - a)/2)$. Because $L > a$, a plateau is observed from $*C$ through $*C*D$ $(-x' = 0)$ to $*D$ $(-x' = (L - a)/2)$. The x' varied from $-(a + L)/2$ to $(a + L)/2$, giving a sine-squared function width of $(a + L)$, including a plateau width of $(L - a)$. See Appendix A.

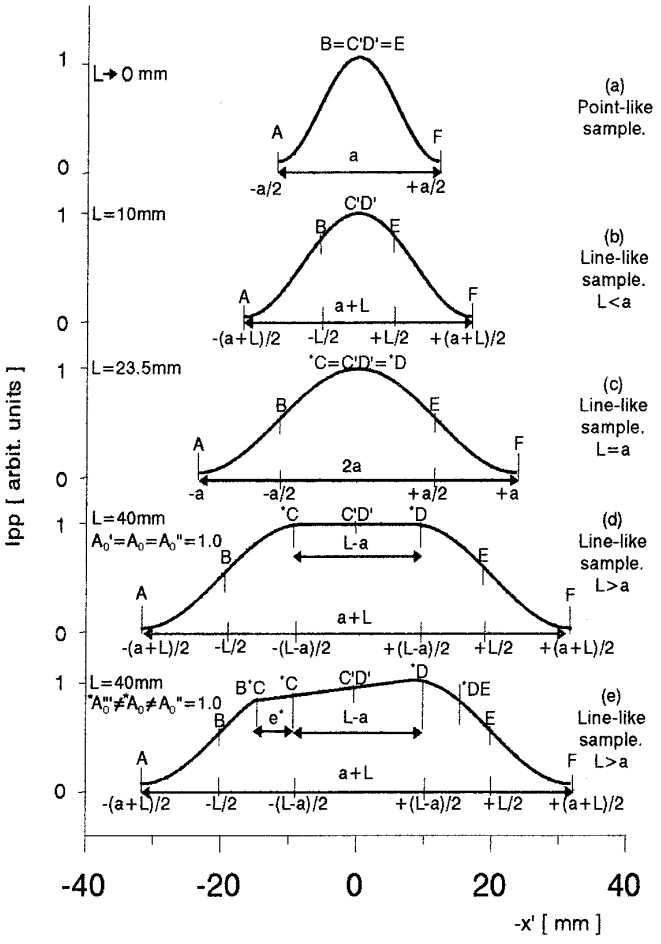

FIG. 2. Variation of the normalized theoretically predicted peak-to-peak height of the first-derivative EPR signal, I_{pp}, as a function of the movement of a line-like sample of variable length, L, along the common sample–cavity x-axis of the rectangular cavity. (a) Point-like sample, $L \rightarrow 0$. (b) Line-like sample, $L < a$. (c) Line-like sample, $L = a$. (d) Line-like sample, $L > a$ (plateau). (e) Line-like sample, $L > a$ (''sloping plateau''). The maximal I_{pp} value was taken as unity. (For the symbol abbreviations and more details see text.)

(iv) A line-like sample with $L > a$, Fig. 2e.

The analysis for this situation is the same as that for the previous case. However, there are clearly differences between the two cases, primarily in that the plateau region is replaced by one in which I_{pp} increases linearly with posi-

tion. As a first approximation, a linear regression model was used for the theoretical prediction of the I_{pp} values over this region. A new auxiliary point B^*C was constructed as the crossing point of the linear function (intercept p and slope q) with the left half of the theoretical sine-squared function (see Appendixes A and B). The I_{pp} values varied in the same way as in case iii, from A ($-x' = -(a + L)/2$) to B^*C. From this point the I_{pp} values increased linearly to the maximum at $^*D$ ($-x' = (L - a)/2$). The sine-squared function width is $(a + L)$, including the linear region, a ''sloping plateau,'' equal to $(L - a + e^*)$, cf. $(L - a)$ for the previous case.

ANALYSIS OF VARIOUS EXPERIMENTAL SITUATIONS

The different combinations of possible experimental situations arising from insertion of the sample into the first and/or second cavity of the double TE_{104} rectangular cavity were reported in Ref. (*12*). The results were found to be the same, if the complementary cavity contained an empty sample tube (i.d. = 1.3 mm), or was completely empty. However, it was demonstrated that the various ways of sample reinsertion, retuning, and remeasurement could significantly affect the measured I_{pp} values (*12*). Consequently the possible influence of sample reinsertion, cavity retuning, and spectral remeasurement on I_{pp} during the experimental monitoring of the movement of line-like samples along the common sample–cavity axis was analyzed. In each of the following cases the sample was inserted at the starting point, the machine was tuned, and the spectrum was recorded. The sample was then moved, using an incremental distance of 2.5 mm, as described.

(1-i) The sample was inserted into the center of the cavity, $S_c(L/2) \equiv P_c(0)$, and then moved down to the lower boundary, $S_L(L) \equiv P_{out}$, and back through the central position to the upper boundary, $S_0(0) \equiv P_{in}$. (1-ii) The reverse of the above took place; starting from the central position, $S_c(L/2) \equiv P_c(0)$, the sample was moved up to the top boundary, $S_0(0) \equiv P_{in}$, and back through the central position to the lower boundary, $S_L(L) \equiv P_{out}$.

(2) The sample was inserted at the top of the active part of the cavity, $S_0(0) \equiv P_{in}$, and then moved down to the lower boundary, $S_L(L) \equiv P_{out}$.

(3) The sample was inserted at the bottom of the active part of the cavity, $S_L(L) \equiv P_{out}$, and then moved up to the upper boundary of the cavity, $S_0(0) \equiv P_{in}$.

(4) Procedures (1), (2), and (3) were repeated; however, the sample was removed/reinserted at positions $S_L(L) \equiv P_{out}$ for (1-i), $S_0(0) \equiv P_{in}$ for (1-ii), $S_c(L/2) \equiv P_c(0)$ for (2), and $S_c(L/2) \equiv P_c(0)$ for (3), at which point the cavity was retuned and the spectra were measured.

The above experiments showed that the dependence of I_{pp} on position was independent of the method by which it was measured. The same trends were observed whether the sample was in the first or the second cavity of the double TE_{104}, and in the single TE_{102} cavity. No observable differences were observed if the complementary cavity of the TE_{104} contained an empty sample tube or was completely empty. However, removal/reinsertion of the sample followed by retuning gave rise to a discontinuity in I_{pp} because the cavity was not identically biased, but the trends remained the same and the effect could be corrected by a simple multiplicative factor.

The I_{pp} values were also measured in the top sample access hole, e (above the sample position $S_0(0) \equiv P_{in}$), and in the lower sample access hole, f (below the sample position $S_L(L) \equiv P_{out}$); however, all I_{pp} values were found to be zero within the experimental error.

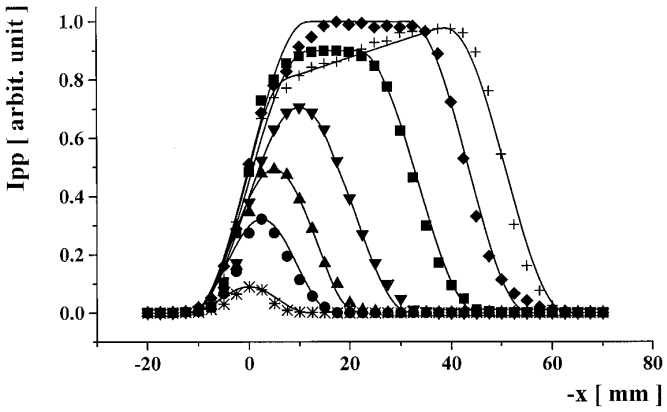

FIG. 3. Variation of the normalized experimentally observed peak-to-peak height of the first-derivative EPR signal, I_{pp}, on the movement of a point-like sample (*), and line-like samples of lengths 5 mm (●), 10 mm (▲), 20 mm (▼), 30 mm (■), 40 mm (♦), and 50 mm (+), along the common sample–cavity x-axis of the first cavity of the double TE_{104} rectangular cavity, and the corresponding theoretically computed dependencies (solid lines) from the theoretical sine-squared function, which was modified for line-like samples with various lengths. The maximal I_{pp} value was taken as unity for all cases. (See Appendixes A and B for further details.)

RESULTS AND DISCUSSION

The I_{pp} values depended strongly on the sample length, sample shape, and sample position within the microwave cavity (*5, 11–22*) and serious systematic errors may be incurred in quantitative EPR spectroscopy if samples with different lengths or internal diameters are compared. These sources of errors can be exacerbated by incorrect positioning of the sample in the microwave cavity. Consequently the variation of I_{pp} values with movement of line-like samples with lengths from 5 to 50 mm along the common sample–cavity x-axis of the first and/or second cavity of the double TE_{104} rectangular cavity has been analyzed. The single TE_{102} rectangular cavity was used for the comparison.

Figure 3 shows how the normalized experimentally observed peak-to-peak height of the first-derivative EPR signal,

I_{pp}, varied with the movement of a point-like sample (∗) and line-like samples with lengths 5 mm (●), 10 mm (▲), 20 mm (▼), 30 mm (■), 40 mm (♦), and 50 mm (+), along the common sample–cavity x-axis of the first cavity of the double TE_{104} rectangular cavity. The maximal I_{pp} value, the averaged I_{pp} value over the plateau region in the case of the 40-mm sample, was taken as unity for all samples. The same trends of the I_{pp} dependencies were obtained for the second cavity of the double TE_{104}, and for the single TE_{102} rectangular cavity. The solid lines in Fig. 3 represent the theoretically computed curves (see Appendixes A and B). The agreement between theory and experiment is good in all cases and any deviations can be attributed to the presence of the sample access holes (*17, 24*), the compression field effect (*5, 19*), and nonuniformity of both the microwave and the modulation fields (*13, 17, 18*) which were not included in the theoretical function. From Fig. 3 it can be concluded that:

(a) For samples with $L < a$ (23.5 mm) the experimental curves can be modeled on the sine-squared function, although there appears to be a slight asymmetry in the experimental results.

(b) For $L > a$, there is a plateau corresponding to the movement of a constant mass of the sample through the cavity; however, prior to the plateau there are systematic differences between the theoretical and experimental results which are more pronounced for the 40-mm sample than for the 30-mm sample. Theoretically the plateau width should be $L - a$; however, in practice the observed values were 7.5 mm (10 mm) and 17.5 mm (17.5 mm) for the 30- and 40-mm samples, respectively, where the figures in parentheses refer to the single TE_{102} cavity. The standard deviations of the averaged I_{pp} values over this region are 0.26% (0.47%) and 1.07% (0.76%) for these two samples. The small deviation of the experimental I_{pp} values prior to reaching the plateau, near $*C$ ($-x = a/2$), is probably caused by a combination of effects arising from microwave and modulation field perturbations at the top and bottom ends of the samples and perturbations caused by the sample access holes (*17, 24*).

(c) For the 50-mm sample the above plateau is replace by a linearly increasing region (sloping plateau), of width 28.5 mm (30 mm), and the linear regression parameters are intercept, $p = 0.86$ (0.83), slope, $q = 0.0065$ mm^{-1} (0.0067 mm^{-1}), and correlation, $r = 0.98$ (0.99), in which I_{pp} depends upon the amount of sample in the inlet and outlet access holes. The theoretically predicted width, $L - a$, is 26.5 mm, which gives $e* = 2$ mm (3.5 mm), and the difference between the maximal and minimal I_{pp} value over this range is 16.51% (17.81%) of the maximal I_{pp} value. Superimposed on this linear region is an oscillating function with a wavelength quite close to the length of the cavity, viz. ≈22.5 mm (22.3 mm), and an average amplitude of 6.11% (6.29%) of the total signal height. Detailed examination of this oscillation shows that it is not a simple sine wave but a quite complex function of x.

(d) The sharp maximum values of I_{pp} for all samples with $L \leq a$ coincide with the central sample position, $S_c(L/2) \equiv P_c(0)$; however, the center of these samples nevertheless must be accurately positioned at the center of the microwave cavity to avoid substantial deviations in measured I_{pp} values. For the 30-mm sample the center of plateau region is practically coincident with the center of the sample at the center of the cavity and this position is recommended for the quantitative EPR measurements although positioning is not as critical in this case. For longer samples, $L = 40$ and 50 mm, optimized values for I_{pp} correspond to the sample center, $S_c(L/2)$, being shifted below the physical center of the cavity.

Some of the above experiments were repeated using the movement of the sample into the first cavity, in the presence of a sample of constant length (e.g., $L' = 30$ mm) fixed in the center of the second cavity, $S'_c(L'/2) \equiv P'_c(0)$. No observable differences were found with the results reported above. In addition the I_{pp} values of the fixed sample in the complementary cavity remained constant within an experimental error of 0.9–1.3% during sample movement in the first cavity and no measurable differences were found when comparing the results after interchanging the moving and fixed samples between the first and second cavity in accordance with our previous results (*12*).

Figure 4a shows the dependence of the experimental I_{pp} values as a function of the sample length, L, for the sample positioned at important points in the rectangular cavity, namely $S_0(0) \equiv P_c(0)$ (▲), $S_0(0) \equiv P_{out}(a/2)$ (▼), $S_c(L/2) \equiv P_c(0)$ (●), and the sample position in the cavity, at which the I_{pp} values were a maximum (■). All the data are taken from Fig. 3. In all cases it is clear that the relationship between I_{pp} and sample length (and hence volume and mass) is nonlinear and for the cases studied the optimum sample length is 40 mm. Figure 4b shows the experimentally determined position in the cavity at which I_{pp} is a maximum as a function of sample length (●). The theoretically predicted dependence (▲) is also shown for the ideal case in which all maximal I_{pp} values are at the central sample position, $S_c(L/2) \equiv P_c(0)$, with ($-x = L/2$) for all samples. For samples with $L \leq a$ the experimental and theoretical curves are coincident; however, for $L > a$ the position of the center of the sample for maximum I_{pp} is moved below the center of the cavity by 1.25, 3.75, and 13.75 mm for the 30-, 40-, and 50-mm samples, respectively.

There is an increasing deviation between the experimental and theoretical curves as the sample length increased. For the optimum sample length, $L = 40$ mm, then, with the center of the sample at the center of the cavity, $S_c(L/2) \equiv P_c(0)$, both ends of the sample protrude outside the active length of the cavity by about 8 mm and, experimentally, as the sample is moved through the cavity a plateau of width

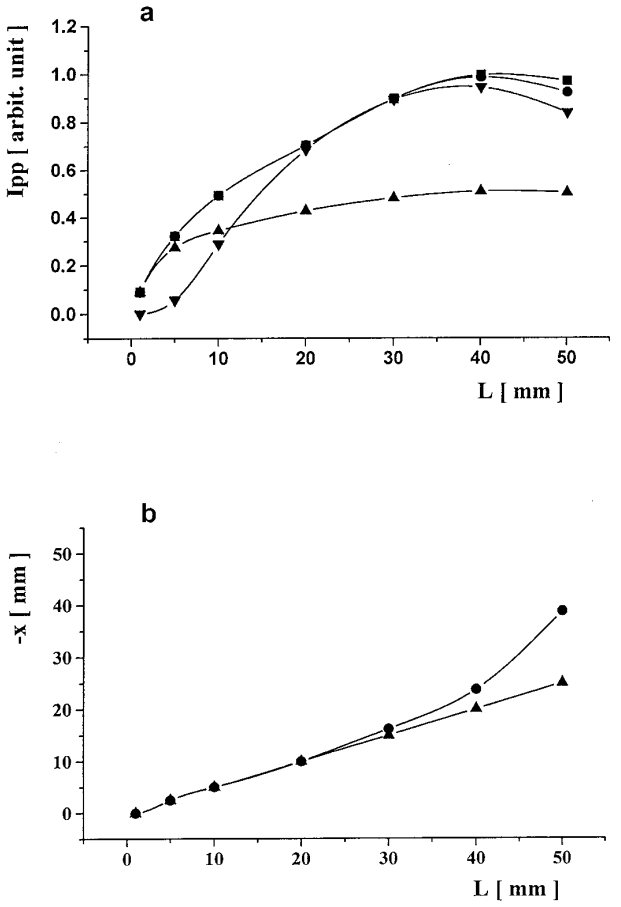

FIG. 4. (a) Variation of the normalized experimentally observed peak-to-peak height of the first-derivative EPR signal, I_{pp}, as a function of the sample length, L, centered at important sample positions in the rectangular cavity: $S_0(0) \equiv P_c(0)$ (▲), $S_0(0) \equiv P_{out}(a/2)$ (▼), the central sample position, $S_c(L/2) \equiv P_c(0)$ (●), and the sample positions in the cavity, at which the I_{pp} values were a maximum (■). If a plateau appeared, then the averaged value of I_{pp} over the plateau region was taken as a maximum. (b) Dependence of the x-coordinate corresponding to the maximum I_{pp}, as a function of the sample length, L. Experimentally observed dependence (●). Theoretically predicted dependence, calculated as $-x = L/2$ (▲). The maximal I_{pp} value was taken as unity for all cases.

17.5 mm is observed. With the 50-mm sample about 13 mm of sample is situated outside the active part of the cavity and the above plateau is replaced by a linearly sloping region. The length of the upper and lower access holes is e = 39.5 mm and f = 46.5 mm (see in Fig. 1). The reason for this is unclear. Probably, the existence of the various lengths of the sample ends in the access holes caused the additive increasing/decreasing of the I_{pp} values by the different additional perturbations of both microwave and modulation fields (*17, 24*).

In order to try to understand the experimentally observed I_{pp} dependence on cavity position, the field compression effect of the various samples situated in the double TE_{104} rectangular cavity was investigated. The field compression factors were evaluated according to the literature (Ref. *5*, p. 4378; Ref. *19*, Eq. [3.22]) with the sample at the central position, $S_c(L/2) \equiv P_c(0)$, of the first cavity and the reference sample, of constant length L' = 30 mm, at the central position, $S'_c(L'/2) \equiv P'_c(0)$, of the second cavity. The results are summarized in Table 2, which shows the experimentally observed dependence of the field compression factors (*f*-factors) as a function of the differences between the sample length in the two cavities, $\Delta L = L - L'$. The reverse situation, the fixed, constant-length sample in the first cavity and variable-length sample in the second cavity, was also measured, shown in parentheses. It is interesting to note that:

(a) The *f*-factors for samples of the same length, ΔL = 0, were 1.01 or smaller, and field compression is thus negligible in this case.

(b) The dependence of the *f*-factors on ΔL is nonlinear; e.g., comparing the *f*-factors for the two combinations with sample lengths (i) L' = 30 mm, L = 10 mm, and (ii) L' = 30 mm, L = 50 mm (the same $|\Delta L|$), it is clear that different *f*-factors were found and those for the larger sample, L = 50 mm, were larger than those for the smaller sample.

(c) For samples with $L < 50$ mm in 1.3-mm tubes the *f*-factors were 1.07 or smaller for all samples. These are similar to values published in the literature; e.g., Casteleijn, and co-workers (*5*) obtained *f*-factors of 1.06 ± 1.89% for an empty EPR sample tube with i.d. = 2.9 mm and 1.15 ± 1.74% for the same tube filled with alanine. Very similar *f*-factors were obtained in the present work for the combination of one EPR tube filled with the strong pitch in KCl (o.d. = 4 mm, L = 100 mm) inserted at the central position of the first cavity, and a second sample (i.d. = 1.3 mm, L' = 30 mm) at the equivalent point in the second cavity, for which the *f*-factor was 1.14 ± 3.52 and 1.16 ± 3.87% after interchanging the samples.

Burns and co-workers (*25*) measured I_{pp} values of DPPH dissolved in toluene and contained in quartz EPR tubes with internal diameters ranging from 1 to 6 mm and tube wall thicknesses from 0.8 to 1.2 mm, and showed that the optimal i.d. was 4 mm for their experimental configuration. Nagy and Plaček (*18*) showed that the spatial dependence of I_{pp} versus a point-like sample movement in the cavity was a very complex function of the sample position. The results, see Figs. 3 and 4 in (*18*), indicate that the radial dependence of the I_{pp} values in the plane, which is situated at the center of the cavity and is perpendicular to the sample movement axis, showed circular symmetry for a sample with i.d. ≤ 2 mm and that all volume elements, ΔV, of this sample within this circle experience the same microwave field. The authors expected an ellipsoidal dependence of the I_{pp} values versus vertical point-like sample positions in the space of the cylinder with the 1-mm radius. This dependence is probably due to strong deformation of the field near the sample access holes (*26*).

As shown in the literature (*5, 13–22*), and also the results presented herein, the sample position in the cavity, sample

TABLE 2

Field Compression Factor (*f*-Factor) as a Function of the Difference in Sample Length, $\Delta L = L - L'$, between Line-like Samples with Variable Lengths, L, Inserted at the Central Position, $S_c(L/2) \equiv P_c(0)$, of the First Cavity and the Reference Sample, $L' = 30$ mm, Inserted at the Central Position, $S'_c(L'/2) \equiv P'_c(0)$, of the Second Cavity of the Double TE_{104} Rectangular Cavity[a]

	ΔL (mm)					
	−25	−20	−10	0	+10	+20
f-factor (a.u.)	1.07 ± 1.15%	1.06 ± 1.75%	1.03 ± 1.15%	1.01 ± 0.69%	1.03 ± 1.57%	1.09 ± 1.69%
	—	(1.07 ± 1.17%)	—	(1.01 ± 0.91%)	—	(1.11 ± 1.76%)

Note. The field compression factor was evaluated according to the literature (5):

$$f\text{-factor} = \{I_{pp} \text{ (with sample in the second cavity)}/I_{pp} \text{ (without sample in the second cavity)}\}_{\text{measured in the first cavity}} \times \{I_{pp} \text{ (without sample in the first cavity)}/I_{pp} \text{ (with sample in the first cavity)}\}_{\text{measured in the second cavity}}.$$

[a] The values in parentheses are from the reverse situation, in which the samples were interchanged between the first and second cavities (averaged values from five experiments).

size, and sample shape can introduce a significant errors in quantitative EPR measurements. The majority of the above-mentioned results were obtained using either a point-like sample (e.g., a very small cube) or a line-like sample with a small internal diameter (e.g., i.d. = 1.3 mm in the present work). However, these are frequently not the ones generally used experimentally. One type of commercially available standard sample (e.g., from Varian or Bruker) is strong pitch in KCl, contained in a thin-walled quartz tube (o.d. ≈ 4 mm). This standard sample is usually inserted such that the pitch extends the full length of the microwave cavity. However, the sample under investigation usually has a different size and shape. Figure 5 shows how the normalized I_{pp} values varied with the movement of such a large cylindrical sample (o.d. ≈ 4 mm, $L \approx 100$ mm) along the common sample−cavity x-axis of the first cavity of the double TE_{104} rectangular cavity (●). The complementary cavity was empty. The same trends were obtained for the second cavity, and for the single TE_{102} cavity. The theoretically predicted dependence (solid line) was calculated using the sine-squared function; see Appendixes A and B. The maximal I_{pp} value was taken as unity for both cases. It is clear that the trends for the experimental and theoretical dependencies are very similar to those obtained for a 50-mm sample discussed with respect to Fig. 3 (+). Therefore only special features will be discussed:

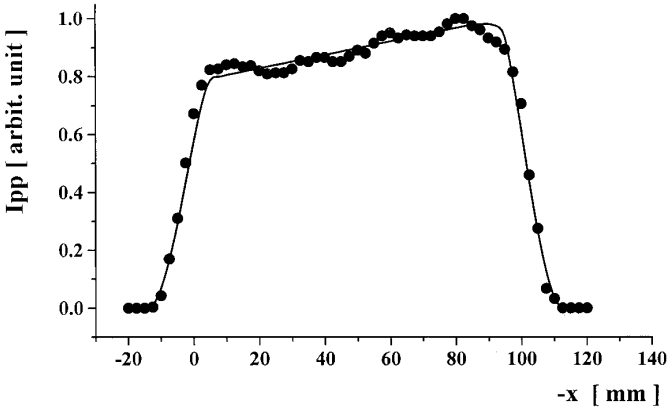

FIG. 5. Variation of the normalized peak-to-peak height of the first-derivative EPR signal, I_{pp}, on the movement of a large cylindrical sample (o.d. ≈ 4 mm, $L \approx 100$ mm) along the common sample−cavity x-axis of the first cavity of the double TE_{104} rectangular cavity. Experimentally observed dependence (●), theoretically calculated dependence (solid line). The maximal I_{pp} value was taken as unity for both cases.

(a) The width of the linear region is 82.5 mm and the linear regression parameters are intercept, $p = 0.78$, slope, $q = 0.0024$ mm^{-1}, and correlation, $r = 0.94$. The theoretically predicted width of a sloping plateau ($L - a$) is 76.5 mm, which gives $e^* = 6$ mm.

(b) The difference between the maximal and minimal I_{pp} in this region is 22.97% of the maximal I_{pp} value, and an average amplitude of the superimposed oscillation is 7.08%, with a wavelength of ≈22.5 mm.

Possible explanations of the I_{pp} oscillations on the linear region may be speculated: (i) it could be due to sample inhomogeneity; this can be discarded since the experiment was repeated with three independent samples (two Varian standards and one Bruker) and each showed a similar effect; (ii) contributions to I_{pp} from those parts of the sample not directly situated in the active part of the cavity (i.e., in the upper and lower sample access holes); and (iii) large perturbations of both the microwave and the modulation fields in the cavity caused by a large cylindrical sample. This is clearly an important factor as the ''effective cavity length'' and the slope of the linear region increase as the sample length increases. Similar, but more pronounced, effects were observed when a 100-mm, 4-mm-diameter sample was inserted in the cavity as described below.

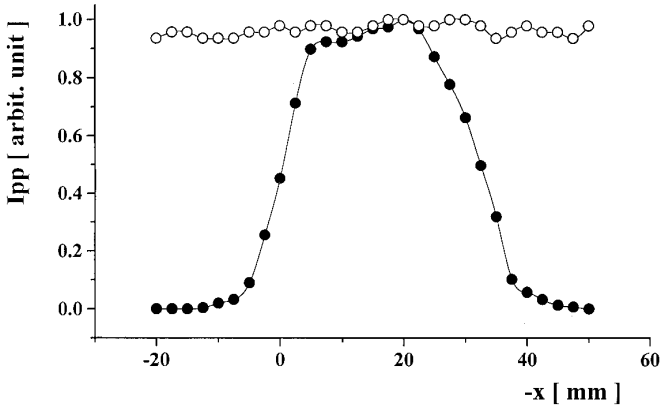

FIG. 6. Variation of the normalized experimentally observed peak-to-peak height of the first-derivative EPR signal, I_{pp}, upon the movement of a line-like sample (i.d. = 1.3 mm, L = 30 mm) along the common sample–cavity x-axis of the first cavity (●), and the simultaneous EPR signal from a large cylindrical sample (o.d. ≈ 4 mm, $L \approx 100$ mm), which was fixed at the central position of the second cavity of the double TE_{104} cavity (○). The maximal I_{pp} value was taken as unity for both cases.

Figure 6 shows how the normalized experimentally observed I_{pp} values varied upon the movement of one of the line-like samples (L = 30 mm, i.d. = 1.3 mm) along the common sample–cavity x-axis of the first cavity (●), in the presence of a large cylindrical sample (i.d ≈ 4 mm, $L' \approx$ 100 mm) which was fixed in the central position, $S'_c(L'/2) \equiv P'_c(0)$, of the second cavity of the double TE_{104} rectangular cavity. The I_{pp} values of a large cylindrical sample fixed in the second cavity were taken simultaneously (○). The maximal I_{pp} value was taken as unity for both cases, and no principal differences were found for the case where the samples were interchanged between the two cavities. It is evident that:

(a) The I_{pp} values of a large cylindrical sample fixed in the second cavity remained constant within an experimental error of 2.67% as a line-like sample was moved through the first cavity.

(b) The I_{pp} dependence of a line-like sample in the first cavity showed very similar trends as were found previously, see Fig. 3 (■), in terms of the width of the plateau; however, the presence of a large cylindrical sample fixed in the complementary cavity caused the previously flat plateau to develop a sloping plateau upon which was superimposed an oscillation similar to that illustrated in Figs. 3 (+) and 5.

(c) The curve has a width of 10.5 mm over the linear region; hence, the theoretically predicted width ($L - a$) is 6.5 mm, which gives $e^* = 4.0$ mm. Linear regression parameters are intercept, $p = 0.87$, slope, $q = 0.0065$ mm^{-1}, and correlation, $r = 0.99$.

(d) The difference between the maximal and minimal I_{pp} value over the sloping region is 10.17%, and the average amplitude of the superimposed oscillation is 3.46%.

This clearly demonstrates that the presence of a large cylindrical sample in the complementary cavity produces: (i) nonnegligible perturbations of the microwave and modulation fields in both of the coupled cavities and (ii) significant deformation of the I_{pp} dependence for a line-like sample in the latter cavity of the double TE_{104} rectangular cavity.

To our knowledge, the precise and systematic analysis of the above-mentioned phenomena and the importance of these error sources on the accuracy and reproducibility of the quantitative EPR spectroscopy have not been discussed in the literature and more attention to the investigation of these, and related phenomena, will be needed in the future.

CONCLUSIONS

The experimentally observed dependencies of I_{pp} on the movement of a line-like sample with length, L, from 5 to 50 mm, along the x-axis of the double TE_{104} cavity, showed: (a) a sharp maximum for the sample length L = 5, 10, 20 mm corresponding to when the center of the sample is situated at the center of the cavity, because the sample length was smaller than the active cavity zone; (b) a plateau with a region, whose width was dependent on the sample length, over which I_{pp} remained constant within experimental errors 0.26–1.07%, for the sample lengths L = 30 and 40 mm because the sample length was greater than the cavity active zone; and (c) for the 50-mm sample this plateau is replaced by a linear region, width 28.5 mm, where I_{pp} is dependent on the position of the sample in the cavity probably caused by combination of the high nonuniformity of both microwave and modulation fields together with contributions to I_{pp} from the inlet and outlet holes of the cavity.

The theoretical predictions of the experimentally observed I_{pp} value dependencies upon the movement of line-like samples with lengths from 5 to 50 mm along the x-axis of the cavity were calculated using the modified sine-squared function. The trends of the experimentally observed and the theoretically predicted dependencies are in very good agreement.

The experimentally observed dependencies of I_{pp} as a function of the sample length are nonlinear, with the maximum I_{pp} values obtained for the 40-mm sample, which is greater than the active length of the microwave cavity, a = 23.5 mm. This may indicate that the existence of the sample in the sample access holes caused the additional increasing/decreasing of the I_{pp} values.

The field compression factors (f-factors) were: (a) negligible, 1.01 or smaller, for identical sample lengths in both cavities; (b) of the order 1.07 or smaller, for the combinations of the 30-mm sample with any of the other samples except for the 50-mm sample, which gave f-factors of 1.09–1.11; and (c) high, 1.14 or more, for the combination of a line-like sample (i.d. = 1.3 mm, $L' = 30$ mm) and a large cylindrical sample (o.d. ≈ 4 mm, $L \approx 100$ mm), which must be taken into consideration, if these two types of the samples are under comparison in quantitative EPR spectroscopy.

The experimentally observed dependence of the I_{pp} values upon the movement of a large cylindrical sample (o.d. $\approx$ 4 mm, $L \approx 100$ mm) along the x-axis of the double TE_{104} cavity showed trends very similar to those found for the line-like sample of $L = 50$ mm. However, the width of the linear region was 82.5 mm ($r = 0.94$), and oscillation of the I_{pp} values around the linear dependence was observed.

The experimentally observed dependence of the I_{pp} values upon the movement of a line-like sample (i.d = 1.3 mm, $L = 30$ mm) along the x-axis of the first cavity of the double TE_{104} cavity in the presence of a large cylindrical sample (o.d $\approx$ 4 mm, $L \approx 100$ mm), which was fixed in the central position of the complementary second cavity, showed that: (a) the presence of a large sample, fixed in the second cavity, caused the additional deformation of the I_{pp} dependence of a line-like sample, which was moving in the first cavity (linearly sloping region occurred, $r = 0.99$); (b) the movement of a line-like sample in the first cavity did not cause any influence on the I_{pp} value dependence of the large sample fixed in the second cavity. The I_{pp} values remained constant within an experimental error of 2.67%.

All the above-mentioned phenomena will give rise to serious sources of significant errors in quantitative EPR spectroscopy, if the samples of identical material to be compared: (i) have different lengths or (ii) have identical lengths but are situated at different sample positions in the cavity.

According to the results obtained it is strongly recommended that the cylindrical samples to be compared in quantitative EPR should have identical length and internal diameter and must be precisely positioned in the microwave cavity.

Finally it should be noted that the results presented herein were obtained on a Bruker ER 200 D-SRC EPR spectrometer, with the original Bruker double TE_{104} and single TE_{102} rectangular cavities. Different EPR spectrometers or cavities could show greater or smaller differences than the results presented herein, and the device given and the experimental configuration used could be characterized with smaller or larger differences.

Detailed analysis of the variation of I_{pp} upon movement of the cylindrical samples with variable internal diameter and sample length, along the x-axis of the double TE_{104} cavity, will be the subject of the next paper.

APPENDIX A

Sine-Squared Function for a Line-like Sample of Variable Length, L

The general equation for the dependence of I_{pp} for a line-like sample of length L along the $-x'$ axis of the microwave cavity is

$$I_{pp}(x') = A_0 \sin^2(\pi/(a + L_{ef})(x' + (a + L_{ef})/2)), \quad [A1]$$

where $A_0 \in \langle 0, 1 \rangle$, and $a = 23.5$ mm for both the Bruker single TE_{102} and the double TE_{104} rectangular cavities.

The general transformation between the x (sample-based) and x' (cavity-based) coordinate systems is

$$x = x' + L/2. \quad [A2]$$

Modification of the General Eq. [A1] for Five Special Cases

(1) Point-like sample ($L \to 0$, $A_0 = 1$). In this case Eq. [A1] simplifies and according to the literature (*13, 17*) is

$$I_{pp}(x') = A_0 \sin^2(\pi/a(x' + a/2)), \quad [A3]$$

where $x' \in \langle -a/2, a/2 \rangle$. Because $L \to 0$, $x' \equiv x$.

(2) Line-like sample ($L < a$, $A_0 = 1$). $L_{ef} = L$, and Eq. [A1] applies

$$I_{pp}(x') = A_0 \sin^2(\pi/(a + L)(x' + (a + L)/2)), \quad [A4]$$

where $x' \in \langle -(a + L)/2, (a + L)/2 \rangle$, and $x = x' + L/2$, for $x \in \langle -a/2, a/2 + L \rangle$.

(3) Line-like sample ($L = a$, $A_0 = 1$). $L_{ef} = a$, and Eq. [A1] applies

$$I_{pp}(x') = A_0 \sin^2(\pi/2a(x' + a)), \quad [A5]$$

where $x' \in \langle -a, a \rangle$, and $x = x' + a/2$, for $x \in \langle -a/2, 3a/2 \rangle$.

(4) Line-like sample ($L > a$, $A_0' = A_0 = A_0'' = 1$), with constant I_{pp} along the plateau. Three special intervals are used:

(i) If $x'' \in \langle -a, 0 \rangle$, then $x'' = x' + (L - a)/2$, for $x' \in \langle -(L + a)/2, -(L - a)/2 \rangle$, and

$$I_{pp}(x'') = A_0' \sin^2(\pi/2a(x'' + a)) \quad [A6]$$

(the left half of the sine-squared function).

(ii) If $*x' \in \langle -(L - a)/2, (L - a)/2 \rangle$, then the plateau region is

$$I_{pp}(*x') = A_0 \ (= A_0' = A_0''). \quad [A7]$$

(iii) If $x''' \in (0, a\rangle$, then $x''' = x' - (L - a)/2$, for $x' \in ((L - a)/2, (L + a)/2\rangle$, and

$$I_{pp}(x''') = A_0'' \sin^2(\pi/2a(x''' + a)) \quad [A8]$$

(the right half of the sine-squared function).

The overall I_{pp} dependence is constructed from Eqs. [A6] and [A8] by the plateau with the constant I_{pp} values, Eq. [A7].

(5) Line-like sample ($L > a$, $*A_0''' \neq *A_0 \neq A_0'' = 1$), with the different $I_{pp}(*x')$ values along the plateau. To a first

approximation, a linear regression model, which included the points $*A_0'''$, $*A_0$, and A_0'', is used for the prediction of the experimental I_{pp} values. The construction of the I_{pp} dependence is a very similar as in the previous case:

(i) If $x'' \in \langle -a, 0)$, $x'' = x' + (L - a)/2$, for $x' \in \langle -(L + a)/2, -(L - a)/2)\rangle$, the same equation as [A6] is used,

$$I_{pp}(x'') = A_0' \sin^2(\pi/2a(x'' + a)). \qquad [A9]$$

where $A_0' = 1$.

(ii) However, if $*x' \in \langle -(L - a)/2, (L - a)/2\rangle$, a linear region is constructed:

$$I_{pp}(*x') = p + q*x'. \qquad [A10]$$

This linear function is projected from the point $A_0'' = 1$ until it intersects with the left half of the sine-squared function, Eq. [A9], at point $B*C$ with I_{pp} $*A_0''' < 1$.

(iii) If $x''' \in (0, a\rangle$, then $x''' = x' - (L - a)/2$, for $x' \in ((L - a)/2, (L + a)/2\rangle$, and the same equation as [A8)] is used,

$$I_{pp}(x''') = A_0'' \sin^2(\pi/2a(x''' + a)), \qquad [A11]$$

where $A_0'' = 1$ and $*A_0$ obeys the relation $*A_0''' < *A_0 < A_0'' = 1$, for the sample positioned at the center of the cavity, $S_c(L/2) \equiv P_c(0)$.

APPENDIX B

Theoretical Prediction of the A_0 Parameter Values in the Sine-Squared Functions

There are two possibilities for obtaining the relative values of A_0: (i) as a first approximation, the maximum of the theoretically predicted I_{pp} can be fitted to the maximum of the experimentally observed I_{pp} (*24*); or (ii) theoretically, using Eq. [6] from Hyde's group's contribution (*27*), which is valid for the samples with $L \leq a$ situated in the center of the X-band rectangular cavity, $S_c(L/2) \equiv P_c(0)$,

$$I(q_0, a, L) \propto \int_{-L/2}^{L/2} \frac{q_0 \cdot \cos^3(\pi(x/a))}{[1 + q_0^2 \cdot \cos^2(\pi(x/a))]^{1/2}} \cdot dx, \qquad [B1]$$

where q_0 is a constant given by Portis (*28*). The combination of both mentioned methods was used in this paper.

Mailer *et al.* (*27*) solved the above integral using numerical integration. We have solved Eq. [B1] analytically (to be published). In both cases it can be shown that the theoretically predicted A_0 value for the X-band Bruker cavity (*23*) with $a = 23.5$ mm is maximal for the sample length $L = a$. However, the above experimental data indicate that the maximum I_{pp} value (corresponding A_0) was obtained for $L = 40$ mm, and the I_{pp} value decreased for the $L = 50$-mm sample. The possible mechanisms causing these differences are unclear.

In an effort to overcome these problems, a new apparent ''a value'' equal to the sample length, L, for which a maximum I_{pp} was experimentally observed, is used in Eq. [B1] for sample lengths $L > a$ (=23.5 mm). For the above data this is $*a = 40$ mm. A possible explanation for the increase in apparent cavity length is that the sample couples the active part of the cavity to both the top, e, and the bottom, f, sample access holes (see Fig. 1e), which then partially contribute to the true length of the microwave cavity. The experimentally observed I_{pp} value, for the sample with $L > a$, situated in the center of the cavity, $S_c(L/2) \equiv P_c(0)$, is subsequently the sum of the partial I_{pp} values from those parts of the sample situated in all three parts of the cavity, and contributions from the sample access holes to the main active part of the cavity cannot be neglected since the differences between the experimentally observed maximal I_{pp} values for sample length $L = 40$ mm (taken as unity) and $L = a$ (=23.5 mm) were found to be about 23%.

Modification of the General Eq. [*B1*] *for Samples of Various Length, L*

(1) Line-like sample, $L \leq a$ (=23.5 mm). The relative values of the A_0 for line-like samples with variable length, L, were calculated using Eq. [B1] with $a = 23.5$ mm ($L = 1.3$ mm for point-like sample).

(2) Line-like sample, $a < L \leq *a$ (=40 mm). The A_0 value was calculated using Eq. (B1) with $a = *a$ (=40 mm). The identity $A_0' = A_0'' = A_0$ was used in the case of a plateau with constant I_{pp}.

(3) Line-like sample, $L > *a$ (=40 mm). The A_0 value was again calculated using Eq. [B1] with $a = *a$ (=40 mm); however, only $*A_0$ can be predicted in this way, and calculation of $*A_0''$ and $*A_0'''$ is not possible. $*A_0''$ and $*A_0'''$ values are approximated by fitting a linear function to the experimental I_{pp} values. $*A_0''$ and $*A_0'''$ are the points of intersection of this linear function, intercept, p, and slope, q, with the right and left half of the sine-squared function, respectively.

(4) In an effort to compare the experimental and theoretically predicted I_{pp} dependencies, the maximum A_0 value (for $L = 40$ mm, and $*a = 40$ mm) was taken as unity for all A_0 parameters, except for $L = 50$ mm. In the case of the sloping plateau, the $*A_0''$ value was normalized, because $*A_0 < *A_0'' < 1$. See previous text and Fig. 2e for more details.

ACKNOWLEDGMENTS

This work was supported by The British Council, Slovakia, and Slovak Grant Agency for Science. We are grateful to Dr. J. Plaček and Professor A. Staško for fruitful discussions during the course of this work. Dr. D. Schmalbein and Dr. P. Such from Bruker Analytic GmbH are acknowledged for valuable information about the properties of modulation field coils in the double TE_{104} cavity and for the signal intensity relationship to sample position for standard Bruker TE_{104} and TE_{102} cavities.

REFERENCES

1. W. Kohnlein, ''Radiation Effects in Physics, Chemistry and Biology'' (M. Ebert and A. Howard, Eds.), p. 206, North-Holland, Amsterdam, (1963).
2. N. D. Yordanov and M. Ivanova, *Appl. Magn. Reson.* **6,** 333 (1994).
3. D. C. Warren and J. M. Fitzgerald, *Anal. Chem.* **49,** 250 (1977).
4. N. D. Yordanov, *Appl. Magn. Reson.* **6,** 241 (1994).
5. G. Casteleijn, J. J. ten Bosch, and J. Smidt, *Appl. Phys.* **39,** 4375 (1968).
6. N. D. Yordanov and M. Ivanova, *Appl. Magn. Reson.* **6,** 347 (1994).
7. D. T. Burns and B. D. Flockhart, *Philos. Trans. R. Soc. London A* **333,** 37 (1990).
8. I. B. Goldberg, H. R. Crowe, and W. M. Robertson, *Anal. Chem.* **49,** 962 (1977).
9. S. C. Blanchard and N. D. Chasteen, *Anal. Chim. Acta* **82,** 113 (1976).
10. I. B. Goldberg, *J. Magn. Reson.* **32,** 233 (1978).
11. M. Mazúr, M. Valko, R. Klement, and H. Morris, *Anal. Chim. Acta* **333,** 249 (1996).
12. M. Mazúr, M. Valko, H. Morris, and Klement, *Anal. Chim. Acta* **333,** 253 (1996).
13. C. P. Poole, ''Electron Spin Resonance: A Comprehensive Treatise on Experimental Techniques,'' Wiley–Interscience, New York (1967).
14. R. S. Alger, ''Electron Paramagnetic Resonance: Techniques and Applications,'' Wiley–Interscience, New York (1968).
15. J. E. Wertz and J. R. Bolton, ''Electron Spin Resonance, Elementary Theory and Practical Applications,'' McGraw–Hill, New York (1972).
16. H. M. Swartz, J. R. Bolton, and D. C. Borg, ''Biological Applications of Electron Spin Resonance,'' Wiley–Interscience, New York (1972).
17. R. C. Barklie and L. Sealy, *J. Magn. Reson.* **97,** 611 (1992).
18. V. J. Nagy and J. Plaček, *Fresenius Z. Anal. Chem.* **343,** 863 (1992).
19. M. L. Randolph, ''Quantitative Considerations in Electron Spin Resonance Studies of Biological Materials. Biological Applications of Electron Spin Resonance'' (H. M. Swartz, J. R. Bolton, and D. C. Borg, Eds.), Chap. 3, pp. 119–153, Wiley–Interscience, New York (1972).
20. P. B. Ayscouth, ''Electron Spin Resonance in Chemistry,'' Methuen, London (1967).
21. D. P. Dalal, S. S. Eaton, and G. R. Eaton, *J. Magn. Reson.* **44,** 415 (1981).
22. M. Sueki, G. A. Rinard, S. S. Eaton, and G. R. Eaton, *J. Magn. Reson. A* **118,** 173 (1996).
23. ''ER Series User's Manual,'' Bruker Analytical Messtechnik GMBH, EPR Division (1983).
24. R. G. Kooser, W. V. Volland, and J. H. Freed, *J. Chem. Phys.* **50,** 5243 (1969).
25. D. T. Burns, M. A. Salem, R. I. Baxter, and B. D. Flockhart, *Anal. Chim. Acta* **183,** 281 (1986).
26. J. Plaček, private communication.
27. C. Mailer, T. Sarna, H. M. Swartz, and J. S. Hyde, *J. Magn. Reson.* **25,** 205 (1977).
28. A. M. Portis, *Phys. Rev.* **91,** 1071 (1953).